14. T. Kitagawa, H. Sakamoto, K. Takeuchi, *J. Am. Chem. Soc.* **121**, 4298 (1999).
15. We find that $C_{60}(CHCl_2)^+$ is produced when $H(CB_{11}H_6Br_6)$ reacts with C_{60} in dichloromethane (Fig. 3C), presumably via protonation of dichloromethane, loss of H_2 to form $CHCl_2^+$, and addition of this carbocation to C_{60}.
16. C. C. Henderson and P. A. Cahill, *Science* **259**, 1885 (1993).
17. G. A. Olah *et al.*, *J. Am. Chem. Soc.* **100**, 6299 (1978).
18. G.-W. Wang, K. Komatsu, Y. Murata, M. Shiro, *Nature* **387**, 583 (1997).
19. Q. Xie, F. Arias, L. Echegoyen, *J. Am. Chem. Soc.* **115**, 9818 (1993).
20. R. C. Haddon, *Acc. Chem. Res.* **25**, 127 (1992).
21. R. Taylor, *Lecture Notes in Fullerene Chemistry* (Imperial College Press, London, 1999).
22. C. A. Reed and R. D. Bolskar, *Chem. Rev.* **100**, 1075 (2000).
23. G. P. Miller, C. S. Hsu, H. Thomann, L. Y. Chiang, M. Bernardo, *Mater. Res. Soc. Symp. Proc.* **247**, 293 (1992).
24. R. D. Bolskar, R. S. Mathur, C. A. Reed, *J. Am. Chem. Soc.* **118**, 13093 (1996).
25. N. G. Connelly and W. E. Geiger, *Chem. Rev.* **96**, 877 (1996).
26. T. Kato *et al.*, *Chem. Phys. Lett.* **180**, 446 (1991).
27. A. J. Bard, A. Ledwith, H. J. Shine, *Adv. Phys. Org. Chem.* **13**, 155 (1976).
28. This paper is dedicated to G. A. Olah who stimulated our interest in carbocations. We thank D. Stasko and N. Fackler for their contributions to this project. Supported by NSF grants CHE-9996002 to C.A.R. and CHE-9982362 to L.J.M. and NIH grant GM23851 to C.A.R.

10 April 2000; accepted 17 May 2000

Subducted Seamount Imaged in the Rupture Zone of the 1946 Nankaido Earthquake

Shuichi Kodaira, Narumi Takahashi, Ayako Nakanishi, Seiichi Miura, Yoshiyuki Kaneda

The Nankai Trough is a vigorous subduction zone where large earthquakes have been recorded since the seventh century, with a recurrence time of 100 to 200 years. The 1946 Nankaido earthquake was unusual, with a rupture zone estimated from long-period geodetic data that was more than twice as large as that derived from shorter period seismic data. In the center of this earthquake rupture zone, we used densely deployed ocean bottom seismographs to detect a subducted seamount 13 kilometers thick by 50 kilometers wide at a depth of 10 kilometers. We propose that this seamount might work as a barrier inhibiting brittle seismogenic rupture.

Large subduction zone earthquakes have repeatedly occurred along the Nankai Trough, in southwest Japan, where the Philippine Sea Plate is subducting beneath Japan. Recurrence intervals and areas affected by these earthquakes have been documented since the seventh century (*1*). According to the historical literature, almost the entire length of the Nankai Trough (500 km) has been ruptured every 100 to 200 years by one or two successive large earthquakes. The most recent events, the 1944 Tonankai and 1946 Nankaido earthquakes, are the best studied of the large Nankai Trough earthquakes (*2*–*5*). The seismic data and geodetic data yield two conflicting results concerning the rupture process of the 1946 Nankaido earthquake. The geodetic data show a rupture area of 2.5×10^4 km^2 with a slip of 5 to 18 m (*3*), whereas the seismic data show a rupture area of 1×10^4 km^2 with a slip of 3 m (*4*). The area of the fault derived from the seismic data corresponds to the 1-day aftershock area (*5*), which is located in the eastern half of the fault area determined by the geodetic data.

We performed a high-resolution deep seismic study in the proposed rupture zone (Fig. 1) to investigate the rupture process of the Nankaido earthquake. We used refraction data generated by a large air gun along a profile (Fig. 1) running in the center of the rupture zone (*2*) at the western edge of the 1-day aftershock area (*5*). To resolve the seismic velocity structure with high resolution to depths of 10 to 30 km, we deployed 98 ocean bottom seismographs (OBSs) with a spacing of 1.6 km on the 185-km-long profile. This spacing of the OBSs is closer than in conventional seismic refraction surveys by a factor of more than 10. All OBSs were positioned at sea bottom by means of a super short baseline (SSBL) acoustic positioning system.

All observed record sections (Fig. 2) showed first arrivals (*P*-wave refraction arrivals) throughout the entire profile, except for OBSs deployed in shallow water

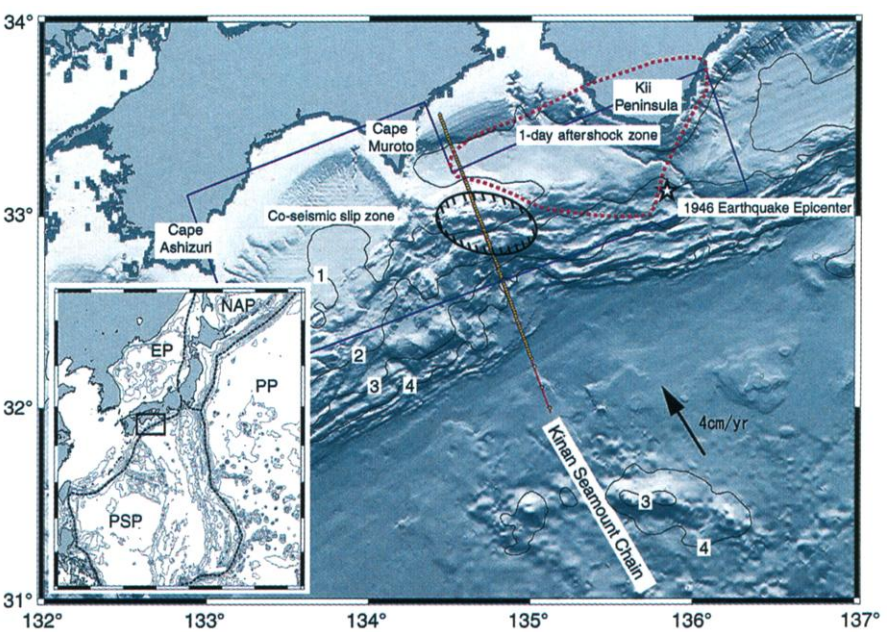

Fig. 1. Topography of the western part of the Nankai Trough and location of high-resolution deep seismic profile. Contour values denote water depth at 1-km intervals. The 1-day aftershock area (*5*) and rupture zone (*2*) derived from geodetic data are shown as dotted and solid lines, respectively. Except for the southern end of the profile, the 98 OBSs (yellow dots) were deployed with 1.6-km spacing. An ellipse on the profile shows the location of the subducted seamount detected by this study. The off-profile dimensions of the seamount are estimated by reference to the size of one of the Kinan seamounts located at the southeastern extension of the profile. The subducted seamount is located immediately outside of the 1-day aftershock zone of the 1946 Nankaido earthquake. The convergence rate of the Philippine Sea Plate under the Eurasian Plate is 4 cm/year (*18*). Topography data used were compiled by the Hydrographic Department, Japan Maritime Safety Agency (*19*). Inset abbreviations: EP, Eurasian Plate; NAP, North American Plate; PP, Pacific Plate; and PSP, Philippine Sea Plate.

Japan Marine Science and Technology Center, Natsushima 2-15, Yokosuka, Kanagawa 237-0061, Japan.

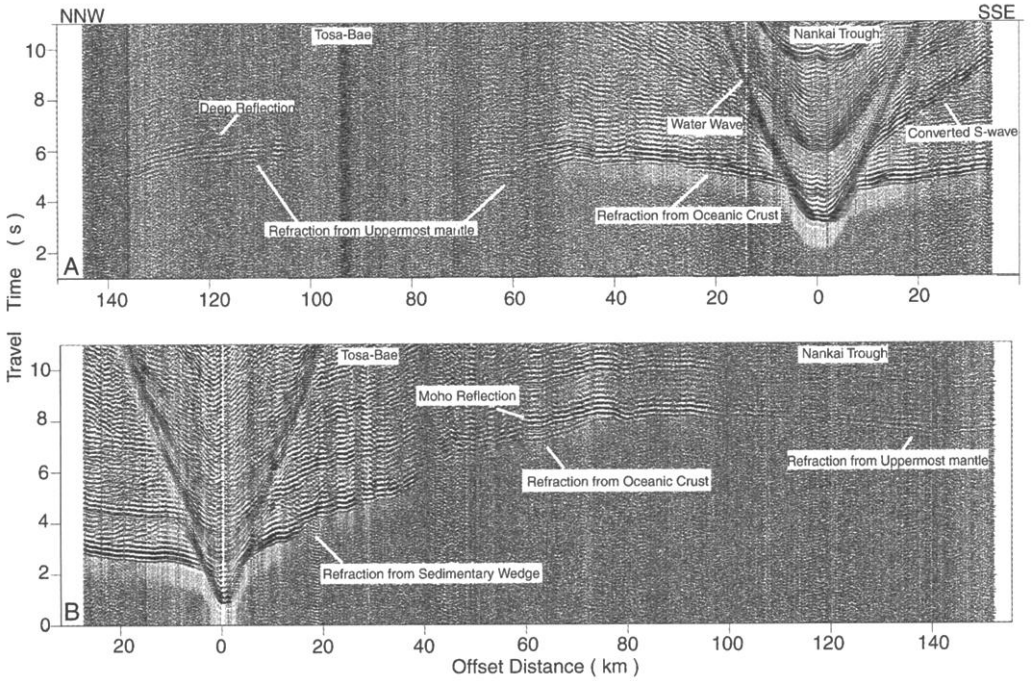

Fig. 2. Examples of observed record section from the vertical component of (**A**) OBS5 and (**B**) OBS81, located at 35 km from the southern end and 28 km from the northern end of the profile, respectively. Vertical axis indicates travel time reduced by 8 km/s. Horizontal axis indicates offset distance from the OBS. A 5- to 20-Hz bandpass filter and automatic gain control with 2-s window are applied. Travel times of all observed refraction phases constitute the input data for the refraction tomography study.

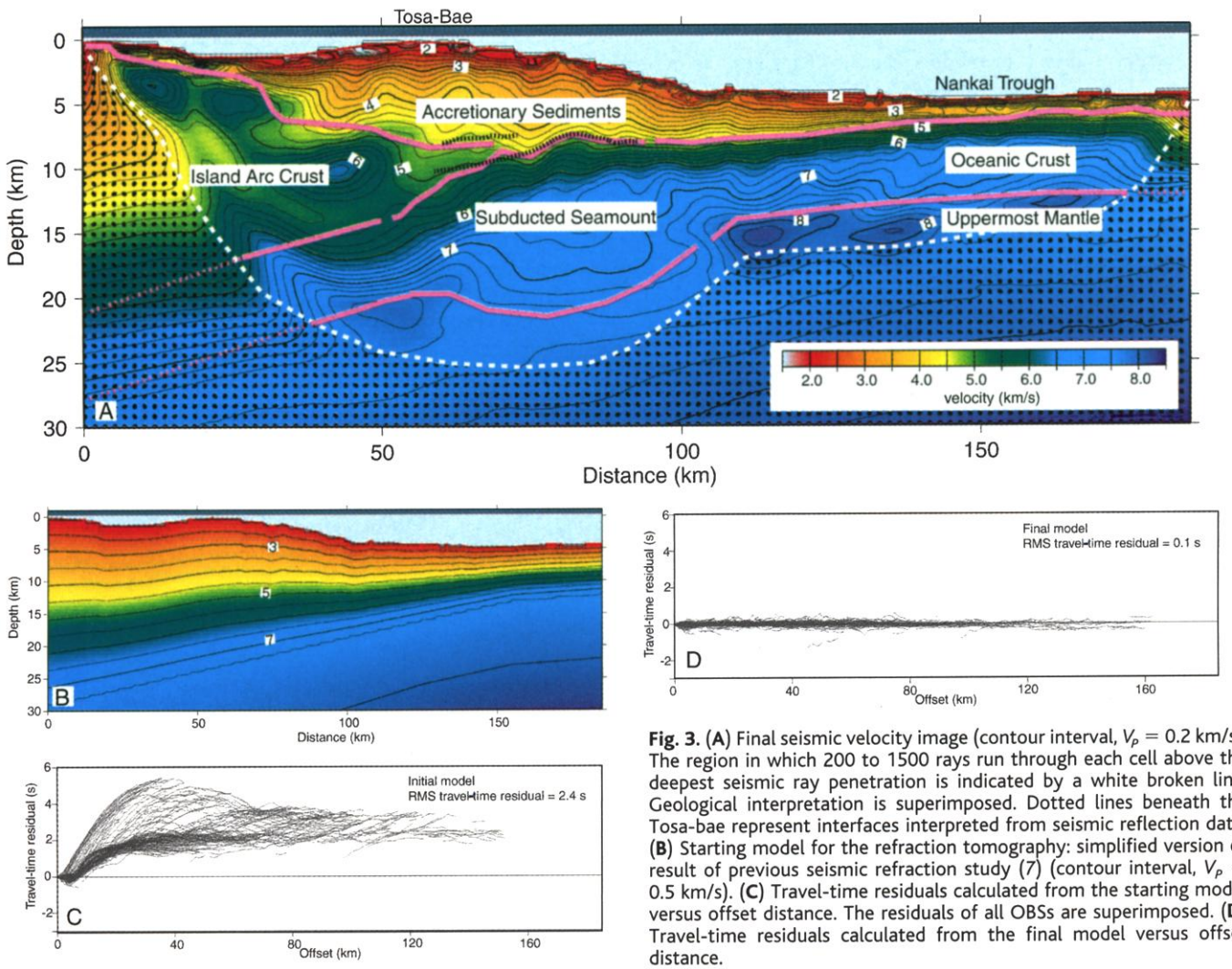

Fig. 3. (**A**) Final seismic velocity image (contour interval, V_P = 0.2 km/s). The region in which 200 to 1500 rays run through each cell above the deepest seismic ray penetration is indicated by a white broken line. Geological interpretation is superimposed. Dotted lines beneath the Tosa-bae represent interfaces interpreted from seismic reflection data. (**B**) Starting model for the refraction tomography: simplified version of result of previous seismic refraction study (7) (contour interval, V_P = 0.5 km/s). (**C**) Travel-time residuals calculated from the starting model versus offset distance. The residuals of all OBSs are superimposed. (**D**) Travel-time residuals calculated from the final model versus offset distance.

(water depth of <200 m). The observed data yielded 44,517 first-arrival picks, from which we determined the *P*-wave velocity (V_P) structure with seismic refraction tomography (*6*). A model was parameterized in 0.5 km by 0.5 km cells. We used a simple landward dipping structure as a starting model (Fig. 3), based on a recent model for the Nankai Trough (*7*). The root mean square (RMS) of the travel-time residual calculated from the starting model is 2.4 s, whereas after the tomographic inversion, the final model (Fig. 3) shows that the RMS residual is reduced to 0.1 s, which is comparable to the uncertainty for the travel-time data (0.02 to 0.10 s).

The final seismic velocity image (Fig. 3) shows two important features: (i) a thick V_P = 5.0 to 7.2 km/s body in the middle of the profile at 25 km seaward from the Tosa-bae topographic high, and (ii) a structure with V_P = 5.0 to 6.0 km/s, which becomes shallower toward the landward end of the profile. The thickness and width of the V_P = 5.0 to 7.2 km/s body are 7 to 13 km and 50 km wide, respectively, and it thins to 6 km on either side. According to previous conventional seismic refraction studies at the northern edge of the Philippine Sea Plate (*7, 8*), *P*-wave velocities of the oceanic crust range between 5.0 and 7.0 km/s with 6 km thickness. The thick 5.0 to 7.2 km/s body in the middle of the model may be locally thickened oceanic crust. Seismic reflection data acquired over the thick V_P = 5.0 to 7.2 km/s body show that the top of the oceanic crust rises 1 to 2 km at the seaward side of the Tosa-bae. The top of the oceanic crust, as interpreted from the seismic reflection data, is plotted on our velocity model.

From these seismic data, we infer the presence of a large-scale subducted seamount 50 km wide and 13 km thick. This conclusion is supported by (i) the existence of the Kinan seamount along the southeastern extension of our profile (*9*), (ii) a magnetic study (*10*) that suggests the possibility of a subducted seamount near the Tosa-bae, and (iii) a landward indentation of the topography that can be recognized seaward of the Tosa-bae (*10*). The shape of this indentation agrees with that obtained from analog modeling of seamount subduction beneath an accretionary prism (*11*). The other notable structure, a region of V_P = 5.0 to 6.0 km/s that thickens to landward, is interpreted as the Japanese island arc upper crust consisting of old accretionary material. Previous seismic refraction studies (*7, 12*) near the Nankai Trough also indicate landward thickening of the Japanese island arc upper crust.

The number of rays running through cells of the model is considered as an index of the reliability of the model. Both features of the velocity structure lie within regions with good ray coverage (Fig. 3), and these features are well resolved. The only areas that are not well constrained by the data are small areas at the western edge and the deepest part of the model. Thus, the model (Fig. 3) resolves a subducted seamount in contact with the Japanese island arc upper crust beneath the Tosa-bae at 10 km depth. We conclude that the seamount is currently colliding with the island arc.

A recent study of tsunami data from the 1946 Nankaido earthquake (*13*) showed a short rise time of the seismic wave in the 1-day aftershock area and slow slip (rise time of 3 to 9 min) in the area to the west of the aftershock zone. Cummins *et al.* (*14*) also concluded that the main earthquake rupture that generated seismic waves is comparable to the 1-day aftershock area and suggested that slow slip occurred along a splay fault cutting through the accretionary sediment to the west of the Tosa-bae. From these two studies, it could be proposed that two phases of the rupture occurred during the 1946 Nankaido earthquake: brittle rupture in the eastern part and slow slip in the western part. Studies of the effect of the buried seamount on the coupling between the plates (*15–17*) suggest that coupling between subducted plate and overriding plate becomes locally stronger because of the subduction of the seamount. From their conclusion (*17*), we propose a possible scenario for the rupture of the 1946 Nankaido earthquake on the basis of our seismic image (Fig. 4): Seismo-tsunamigenic brittle rupture starting off the Kii peninsula stopped beneath the Tosa-bae because of strong coupling at the large subducted seamount; then, only tsunamigenic slow slip propagated from beneath the Tosa-bae to the west off cape Ashizuri.

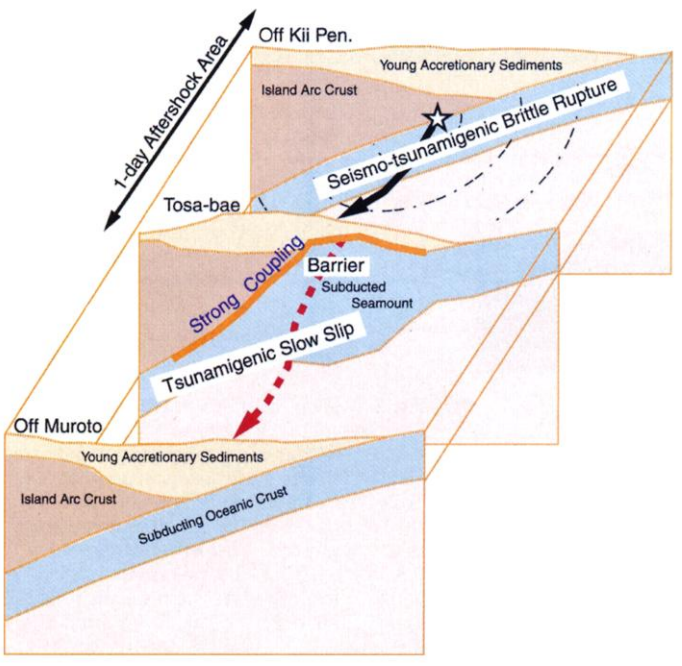

Fig. 4. Schematic diagram of a proposed rupture process of the 1946 Nankaido earthquake on the basis of the seismic velocity image. Previous seismic refraction studies off the Kii peninsula (*12*) and Muroto (*7*) show smooth subduction of the oceanic crust without any structural irregularity such as the large seamount imaged in this study.

References and Notes

1. Y. Kanaori, S. Kawakami, K. Yairi, *Engineer. Geol.* **33**, 289 (1993).
2. M. Ando, *Tectonophysics* **27**, 63 (1975).
3. T. J. Fitch and C. H. Scholz, *J. Geophys. Res.* **76**, 7260 (1971).
4. H. Kanamori, *Phys. Earth Planet. Inter.* **5**, 129 (1972).
5. K. Mogi, *Bull. Earthquake Res. Inst.* **46**, 175 (1968).
6. C. Zelt and P. J. Barton, *J. Geophys. Res.* **103**, 7187 (1998).
7. S. Kodaira *et al.*, *J. Geophys. Res.* **105**, 5887 (2000).
8. H. Kinoshita and M. Matsuda, *J. Geomagn. Geoelectr.* **41**, 161 (1989).
9. K. Kobayashi, S. Kasuga, K. Okino, in *Backarc Basins: Tectonics and Magmatism*, B. Taylor, Ed. (Plenum, New York, 1995), pp. 381–405.
10. T. Yamazaki and Y. Okamura, *Tectonophysics* **160**, 207 (1989).
11. S. Domingues, S. E. Lallemand, J. Malaveielle, R. von Huene, *Tectonophysics* **293**, 207 (1998).
12. A. Nakanishi *et al.*, *Eos* **80** (fall suppl.), 570 (1999).
13. T. Kato and M. Ando, *Geophys. Res. Lett.* **24**, 2055 (1997).
14. P. R. Cummins, Y. Kaneda, T. Hori, S. Hirano, *Eos* **80** (fall suppl.), 738 (1999).
15. J. Kelleher and W. McCann, *J. Geophys. Res.* **81**, 4885 (1976).
16. M. Cloos and R. Shreve, *Geology* **24**, 107 (1996).
17. C. H. Scholz and C. Small, *Geology* **25**, 487 (1997).
18. T. Seno, S. Stein, A. E. Gripp, *J. Geophys. Res.* **98**, 17941 (1993).
19. A. Asada and K. Okino, *Proc. Jpn. Soc. Marine Surv. Technol.* **10**, 15 (1998).

20. We thank the captain, crew, and technical staff of the R/V *Kaiyo*; K. Obana for preparation of OBSs; and T. Tsuru, J.-O. Park, P. Cummins, K. Suyehiro, Y. Kono, and H. Kinoshita for valuable discussions.

21 March 2000; accepted 22 May 2000